

# INTERNATIONAL SOCIETY FOR SOIL MECHANICS AND GEOTECHNICAL ENGINEERING



*This paper was downloaded from the Online Library of the International Society for Soil Mechanics and Geotechnical Engineering (ISSMGE). The library is available here:*

<https://www.issmge.org/publications/online-library>

*This is an open-access database that archives thousands of papers published under the Auspices of the ISSMGE and maintained by the Innovation and Development Committee of ISSMGE.*

*The paper was published in the proceedings of the 10th International Conference on Physical Modelling in Geotechnics and was edited by Moonkyung Chung, Sung-Ryul Kim, Nam-Ryong Kim, Tae-Hyuk Kwon, Heon-Joon Park, Seong-Bae Jo and Jae-Hyun Kim. The conference was held in Daejeon, South Korea from September 19<sup>th</sup> to September 23<sup>rd</sup> 2022.*

## Centrifuge modeling of the deformation of slopes with earthquake-induced cracks during rainfall

J. Xu, K. Ueda & R. Uzuoka

*Disaster Prevention Research Institute, Kyoto University, Japan*

**ABSTRACT:** Earthquake and rainfall are two common natural disasters in many mountainous areas. It has been found in past studies that although earthquake tended to induce cracks on the slope surface, a lot of slopes could still stay stable after earthquake and it was the post-earthquake rainfall that resulted in the final failure of those slopes. Thus, the detrimental effect of the cracks caused by earthquake on the slope stability during rainfall needs to be studied, but a thorough investigation into the slope failure mechanism has not been conducted until now. To evaluate the response of slopes to post-earthquake rainfall, this study performed several centrifuge experiments on unsaturated soil slopes, which were subjected to earthquake and/or rainfall. The earthquake was simulated by shaking excited on the shaking table in the geotechnical centrifuge and the rainfall was simulated by water sprays from nozzles fixed above the slope models. Experimental results revealed that cracks occurred near the slope shoulder during earthquake, and the presence of the cracks significantly affected the features of slope failure caused by the following rainfall, indicating the significance of the shaking effect on the response of slope to rainfall. In addition, when subjected to post-earthquake rainfall, the slope exhibited deformation largely dependent on the rainfall intensity, suggesting that the rainfall intensity played a critical role in the landslide caused by post-earthquake rainfall.

**Keywords:** centrifuge modeling, slope deformation, earthquake-induced cracks, rainfall.

### 1 INTRODUCTION

Earthquakes and rainfall are two common disasters leading to landslides (Keefer 1984; Schuster et al. 1996; Crosta 2004; Sassa et al. 2015) in a lot of mountainous areas in the world. Previous studies mainly focused on landslides or slope stability under a single disaster, either earthquakes or rainfall, which have provided valuable reference for landslide-related prediction and prevention and have been adopted by numerous researchers to investigate the response of slopes to earthquakes or rainfall.

However, the combined effect of natural disasters such as earthquakes and heavy rainfall also constantly poses a threat to some areas. In some cases, slopes with certain topographies or geological conditions have adequate stability under normal static conditions, but become unstable when struck by horizontal forces from earthquakes, inducing cracks on their surfaces rather than failures, making them vulnerable to rainfall.

Increasing attention is being paid to this type of slope failure since it has been reported in the last several earthquakes, such as 2008 Sichuan Earthquake (Tang et al. 2011) and 2011 Tohoku Earthquake (Usui et al. 2013). However, these investigations were preliminary based on aerial images; more detailed research of the slope failure mechanism was highly demanded in order to understand this kind of landslide. Quantitative analysis

in detail such as physical experiment (Xu et al., 2022a) and numerical simulation (Xu et al., 2022b) are needed to assess this phenomenon.

In this study, physical experiments on centrifuge model slopes were performed where earthquakes and rainfall were simulated. The main objective was to investigate the failure triggering mechanism of slopes subjected to post-shaking rainfall.

### 2 SCALLING LAWS IN CENTRIFUGE MODELING

The geotechnical centrifuge applies an increased “gravitational” acceleration to a physical soil model so that the same self-weight stresses in the model and prototype are achieved. The scale model of the prototype has macroscopic dimensions reduced by a factor  $N$  and the same mass density as the prototype. When it is subjected to a centrifugal acceleration equivalent to  $N$  times the Earth’s gravity  $g$ , the stress similarity is achieved at homologous points in both model and prototype. Table 1 contains the scaling factors for common parameters in centrifuge model tests.

Table 1. Centrifuge scaling laws ( $N$  is the centrifugal acceleration).

Parameter	Scale factor (model/prototype)
Stress	1
Length	$1/N$
Acceleration	$N$
Time (dynamic)	$1/N$
Time (static)	$1/N$
Rainfall intensity	$N$
Suction	1

### 3 TEST PROGRAM

Four tests (A1, A2, B1, and B2) were carried out at the centrifuge in the Geotechnical Centrifuge Center, Disaster Prevention Research Institute (DPRI), Kyoto University. This study aimed to examine the effect of shaking-caused cracks on the slope response to the subsequent rainfall. All 1:50 scale model slopes illustrated in Fig. 1 were exposed to a centrifugal acceleration field of 50  $g$  in the process of testing.

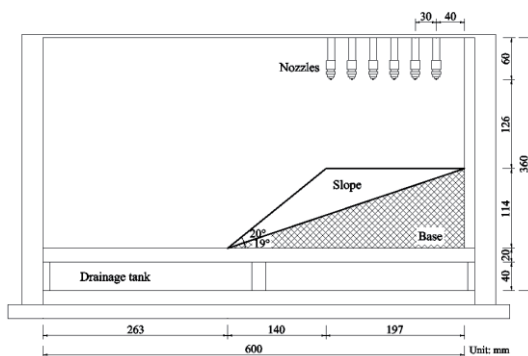


Fig. 1. Centrifuge slope model.

The description of each model test is given in Table 1. Upon the achievement of designated centrifugal acceleration of 50  $g$  in tests A1 and B1, the inflight rainfall simulator was turned on in the container that accommodated the model slope, whereas shaking with a target intensity of 230  $m/s^2$  (4.6  $m/s^2$  in the prototype scale) was excited to the models in tests A2 and B2 prior to rainfall.

Table 2. Centrifuge model test program.

Test	Shaking intensity	Rainfall intensity	External condition for slope
A1	None	30 mm/h	Heavy rainfall
B1	None	9 mm/h	Light rainfall
A2	4.6 $m/s^2$	30 mm/h	Shaking and heavy rainfall
B2	4.6 $m/s^2$	9 mm/h	Shaking and light rainfall

## 4 MODEL SLOPE

### 4.1 Soil property

The soil used for making the slope in this study was decomposed granite soil consisting of a certain amount

of silt. The uniformity coefficient  $C_u$  and curvature coefficient  $C_c$  were calculated to be 7.46 and 1.01 from the particle size distribution curve in Fig. 2a; the fines content was about 10%.

The soil was named well-graded sand with silt (SW-SM) according to the American Society for Testing and Materials classification system. The compaction curve is plotted in Fig. 2b.

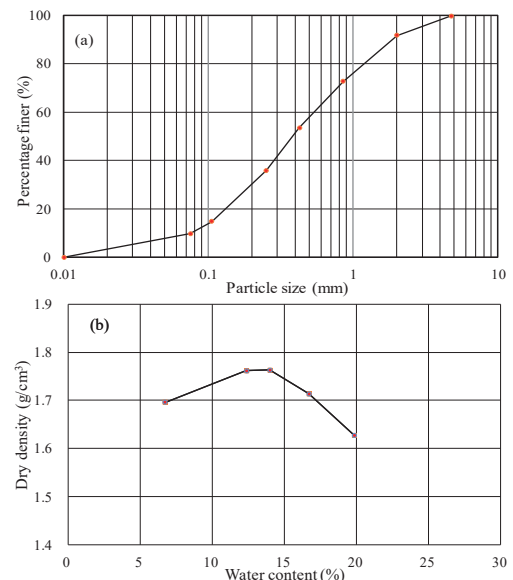


Fig. 2. Soil properties: (a) particle size distribution and (b) compaction curve.

### 4.2 Model preparation

The stepwise moist-tamping technique was employed to prepare the slope models. Water instead of other viscous fluid was used as the experimental fluid to prepare model slopes and simulate rainfall in all the tests; this was because liquefaction was unlikely to occur in slopes during shaking if initial high suction existed in slopes after compaction. Horizontal lines of various heights and the final slope line were delineated on the inside of the container's transparent wall; compaction of soil layer by layer and placement of sensors at the corresponding positions were then performed. In each layer of soil, the water content is 10% and the degree of saturation is 0.35. Once the compaction was completed, excess soil was scraped away.

### 4.3 Instrumentation

During the preparation of the models, accelerometers were put inside the model and markers along the profile. The layout of accelerometers and markers is given Fig 3, the results of accelerations recorded by accelerometers and soil displacement represented by markers would be discussed in the following sections.

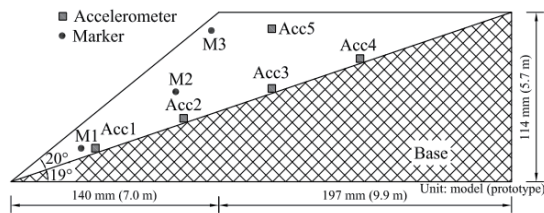


Fig. 3. Layout of accelerometers and markers in the centrifuge model slope.

## 5 TEST RESULTS

The results obtained from the shaking tests in tests A2 and B2 would be introduced before the those from the rainfall tests. Acceleration response and slope deformation due to seismic loading were discussed in the shaking test section; soil displacement and slope deformation were discussed in the rainfall test section.

### 5.1 Response of slope to shaking

The sinusoidal wave with a frequency of 50 Hz (1 Hz in the prototype scale) and a duration of 0.8 s (40 s in the prototype scale) was excited to the container on the shaking table once the centrifugal acceleration went up to 50 g in tests A2 and B2.

To better visualize the acceleration response of the slope in different parts, this section plots the maximum acceleration recorded in both tests. Since the two slopes had the same condition, the comparison of the acceleration can also be used to check the repeatability of the shaking test. Fig. 4 plots the recorded maximum accelerations during shaking in tests A2 and B2.

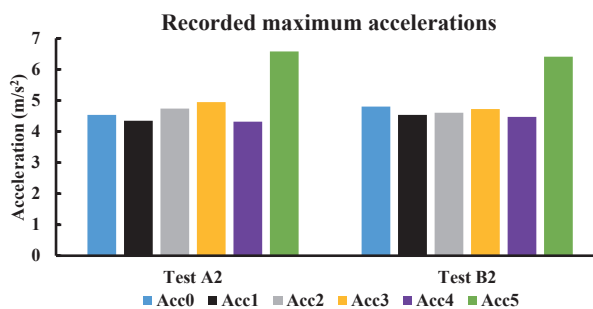


Fig. 4. Recorded maximum accelerations in slopes during shaking in tests A2 and B2.

The acceleration response was consistent in both tests as each accelerometer shows very close value in each test. The amplification effect exhibited by the greatest peak acceleration in accelerometer A5 in each test was also reflected in Fig. 4.

The soil displacement and the distribution of crest cracks in slopes after shaking are presented in Fig. 5. The displacement vectors in Fig. 5a and b clearly show that the soil near the slope surface moves most. The settlement near the slope shoulder is obvious as indicated by the comparison between red line and black line,

which represent the slope outline after and before shaking.

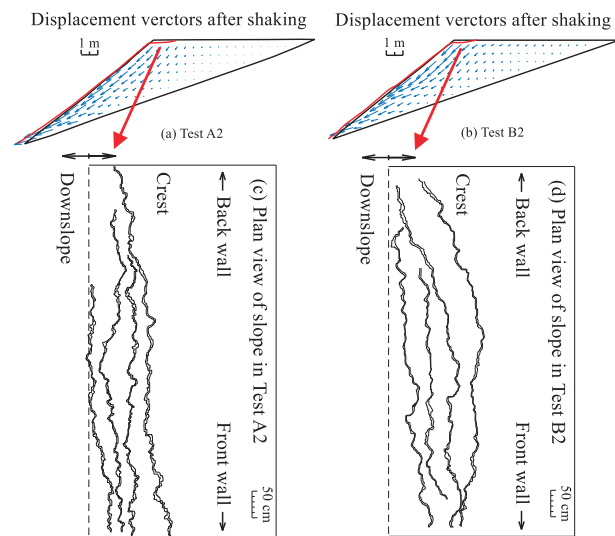


Fig. 5. Displacement vectors after shaking in tests A2 (a) and B2 (b) and crack distributions (c) and (d). (after Xu et al., 2022)

Due to the discontinuity in soil displacement, cracks were generated near the slope shoulder and are located within the area covered by the horizontal red line. With the image analysis, the distribution of cracks due to shaking are illustrated in Fig. 5c and d.

The existence of these cracks greatly affected the slope response to the subsequent rainfall, which would be discussed in the next section.

### 5.2 Response of slope to post-shaking rainfall

To study the effect of the previous shaking on the slope response to rainfall, this section would examine the difference of soil displacement and slope deformation between tests with only rainfall and tests with post-shaking rainfall, i.e., tests A1/B1 and tests A2/B2.

Fig. 6 provides the displacement of soil at three different locations in the slopes during rainfall. Landslide kinematic was analyzed based on the time history of soil displacement. The soil displacement had different patterns in two test series and the effect of shaking-induced cracks on soil displacement depended on the rainfall intensity.

Soil displacement of the slope during post-shaking heavy rainfall, as displayed in Fig. 6a, b, and c, was larger, in comparison with that of the slope during heavy rainfall without antecedent shaking. The shaking-induced crest cracks resulted in a severe and speedy landslide caused by the following rainfall.

However, soil displacement of the slope during post-shaking light rainfall was similar, either in the magnitude or the velocity, to that of the slope during light rainfall without antecedent shaking. This was reflected in Fig. 6d, e, and f. The growth rates of displacement in both slopes

during rainfall, as well as the travel speed of soil, were very similar in both tests.

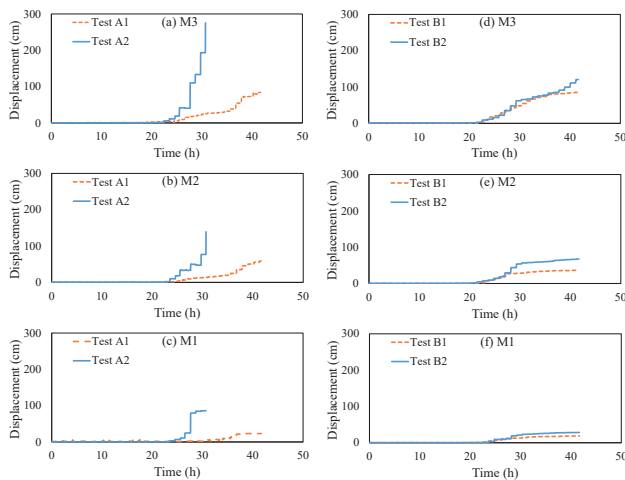


Fig. 6. Soil displacement in slopes in tests A1 and A2, (a), (b), and (c), and tests B1 and B2, (d), (e), and (f)

The progressions of landslides in centrifuge model tests were captured by the front high-speed camera. The images of slopes after failures caused by rainfall in four tests are given in Fig. 7.

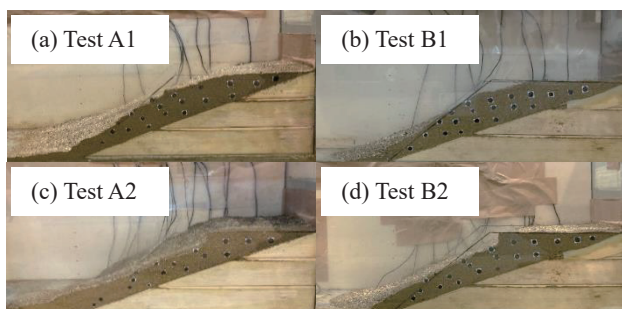


Fig. 7. Images of slope failures caused by rainfall in tests without shaking, A1 (a) and B1 (b), and tests with shaking A2 (c) and B2 (d). (After Xu et al., 2022a)

From the slope profiles after testing, the features of landslides with different external conditions could be easily understood. The landslide profiles in slopes subjected to post-shaking rainfall (Fig. 7c and d) were different from those in slopes subjected to only rainfall (Fig. 7a and b). Also, the landslide features of the slope with shaking-induced cracks were dependent on the rainfall intensity through the comparison of Fig. 7c and Fig. 7d.

## 6 CONCLUSIONS

Four centrifuge model tests on 1:50 scale model

slopes have been carried out to investigate the response of unsaturated slopes subjected to rainfall when they were exposed to antecedent shaking and evaluate the corresponding landslide triggering mechanisms. It was found that shaking-induced crest cracks on the slope were near its shoulder, and these cracks greatly affected slope behavior during the following rainfall.

In addition, heavy rainfall greatly accelerated the failure of the slope with shaking-induced cracks, resulting in a rapid and massive landslide. However, the light rainfall with a lower intensity did not cause significant differences in the slope deformation and landslide kinematics compared to these of the slope subjected to only light rainfall.

Remedies such as covering the cracks or arranging drains at the slope toe area are necessary once an earthquake induces tensile cracks in a slope. It will be effective to restrain the occurrence of sudden slope failure and win time for the evacuation of residents living at the bottom of the slope.

## ACKNOWLEDGEMENTS

This work was supported by JSPS KAKENHI Grant Number 21H04575.

## REFERENCES

- Crosta, G.B. 2004. Introduction to the special issue on rainfall-triggered landslides and debris flows. *Engineering Geology*, 73(3-4), 191-192.
- Keefer, D.K. 1984. Landslides caused by earthquakes. *Bulletin of Geological Society of America*, 95, 406-421.
- Sassa, K., Tsuchiya, S., Fukuoka, H., Mikos, M., and Doan, L. 2015. Landslides: review of achievements in the second 5-year period (2009–2013). *Landslides*, 12(2), 213-223.
- Schuster, R.L., Nieto, A.S., O'Rourke, T.D., Crespo, E., and Plaza-Nieto, G. 1996. Mass wasting triggered by the 5 March 1987 Ecuador earthquakes. *Engineering Geology*, 42(1), 1-23.
- Tang, C., Zhu, J., Qi, X., and Ding, J. 2011. Landslides induced by the Wenchuan earthquake and the subsequent strong rainfall event: A case study in the Beichuan area of China. *Engineering Geology*, 122(1-2), 22-33.
- Usui, Y., Shimada, H., Innami, H., Amao, H., Higashi, K., and Kawabata, H. 2013. Case study on heavy rainfall-induced reactivation of seismically disturbed slope caused by the 2011 off the Pacific Coast of Tohoku Earthquake. In K. Ugai, H. Yagi, and A. Wakai (eds), *Earthquake-Induced Landslides*: 323-329. Springer, Berlin, Heidelberg.
- Xu, J., Ueda, K., and Uzuoka, R. 2022a. Evaluation of failure of slopes with shaking-induced cracks in response to rainfall. *Landslides*, 19 (1), 119-136.
- Xu, J., Ueda, K., and Uzuoka, R. 2022b. Numerical modeling of seepage and deformation of unsaturated slope subjected to post-earthquake rainfall. *Computers and Geotechnics*, 148, 104791.